MODELLING AND TESTING OF ADVANCED INTAKE AND EXHAUST SYSTEM COMPONENTS FOR RACE CAR ENGINES

Booklet of PhD Theses

PREPARED BY:

BARHM ABDULLAH MOHAMAD

Fuel and Energy Engineering (BTech),
Mechanical Engineering Powertrain (MTech)

ISTVÁN SÁLYI DOCTORAL SCHOOL OF MECHANICAL ENGINEERING SCIENCES
TOPIC FIELD OF MECHANICAL ENGINEERING SCIENCES
TOPIC GROUP OF DESIGN OF MACHINES AND ELEMENTS

HEAD OF DOCTORAL SCHOOL
Dr. Gabriella Bognár
DSc, Full Professor

Head of Topic Group
Dr. Gabriella Bognár
DSc, Full Professor

Scientific Supervisor
Dr. Károly Jálics
PhD, Associate Professor

Miskolc
2021

JUDGING COMMITTEE

chair:

secretary:

members:

OFFICIAL REVIEWERS

1. INTRODUCTION

1.1. Motivation

In a race car powered by an internal combustion engine, the quintessential element defining the character of the race car is the engine. The common intake and exhaust system of the engine has improved significantly over the years; therefore, the issue now is more about the quality of the sound of the engine than its noisiness. The identification and the features of sound power emitted by engine components is an important challenge for the race car industrials. Noise generated in interior and exterior parts of the race car grew together with racetrack requiring better noise absorbing technology (Krebber et al. 2002; García and Faus, 1991) .

The noise generated in the intake system as a result of the high velocity of air streaming into the engine combustion chamber increased to the point that rules were needed to prevent the negative impacts of race car noise pollution. Recently, they have been amended to apply a tougher restriction, and the European Union's Environment Action Programme to 2020 proposed a large reduction in noise pollution, almost reaching the World Health Organization's recommended noise levels (Juraga et al. 2015). One of the pieces of equipment used to reduce noise in the circumstances mentioned above is the vehicles intake and exhaust plenum. Positioned at the upstream and downstream of an internal combustion engine (*ICE*) such as intake manifold and exhaust system include filters, exhaust manifold, intercooler, catalist convertor and mufflers are an engineering solution to control engine noise levels and combustion emissions. Increasingly sophisticated modelling methods assist acoustic research and upgrade work on intake and exhaust systems . Such techniques include *1D* gas dynamic simulation codes with the choice to model some components in *3D*. These can provide accurate outputs within a reasonable calculation period.

1.2. Objectives

i. The objective of this research work is the selection, tuning and development of the intake manifold for a Formula Student race car in accordance with the Formula Student regulations. For this purpose, a four-cylinder Honda motorbike engine was chosen by the "Engine Team". Therefore, the first task was to enhance the air flow, resp. to provide sufficient amount of air to the combustion inside the cylinder at higher rpm and reduce the shock waves which may lead to higher sound pressure.

ii. There are secondary injectors on the intake manifold in the original engine, which work as nitro or fuel booster to the air to create rich air to fuel mixture at high engine speed (over *8000 rpm*) and providing only *1 hp* according to the dynamometer. The task is to

remove these secondary injectors and rebuilt the entire intake manifold. This may compensate the power loss due to removing secondary injectors.

iii. Design a proper exhaust system (exhaust manifold, muffler, junctions) for the current formula race car to sustain the critical operation condition.

iv. Simulation and analysing the fluctuation and the uniformity of the flow along the system.

v. Prediction of the emitted noise, generated by the pulsating flow from the intake and exhaust of the system ducts, by using *CFD* (Computational Fluid Dynamics) techniques.

vi. Energy losses troubleshooting by diagnose the heat losses from entire engine block systems.

2. METHODOLOGY

2.1 Geometrical model

In the first part of my dissertation research work I defined the geometry of the region of interest: the computational domain. Because of its convenience and minimal computing costs in the representation of complex geometries, one-dimensional linear acoustic models are extensively used to evaluate the noise performance of intake systems.

Honda CBR 600RR (PC 37) intake manifold *3D* geometry was sketched based on real dimensions using advanced design software Creo 4 see the figure 1 (a, b, c).
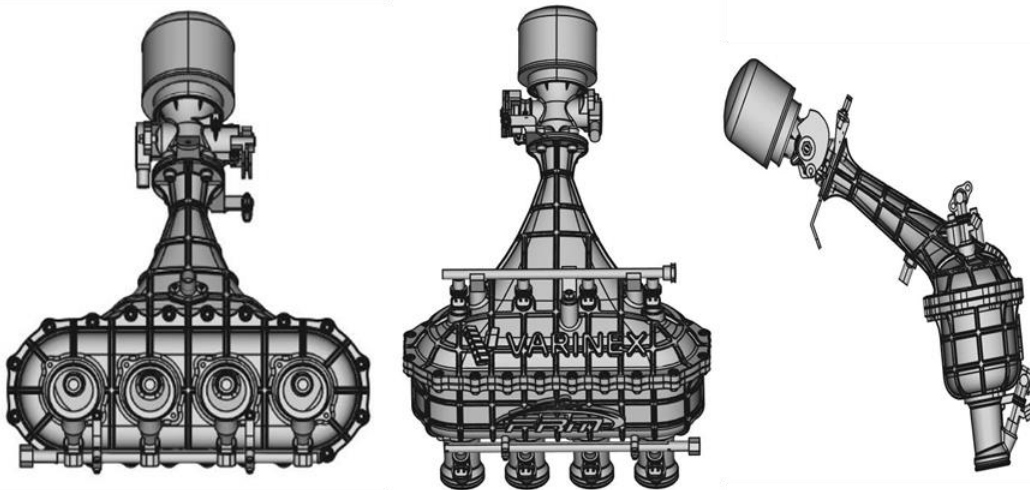

Figure 1 Honda engine Intake manifold *3D* geometry along with restricted, primary injectors and secondary injectors.

To implement the calculation, the AVL package software was used included Boost and *3D* Fire solvers, based on finite volume method and those two solvers were coupled to indicate boundary conditions between virtual engine scheme and valid part of engine (Intake manifold). Every part of the manifold in the AVL simulation software can be described by the inlet diameter, the outlet diameter, the length, the wall thickness, the material and friction

and heat transfer coefficients as in figure 2. Values of pressures and temperatures for the individual cylinders of the engine in relation to time were subsequently generated from the *1D* model .
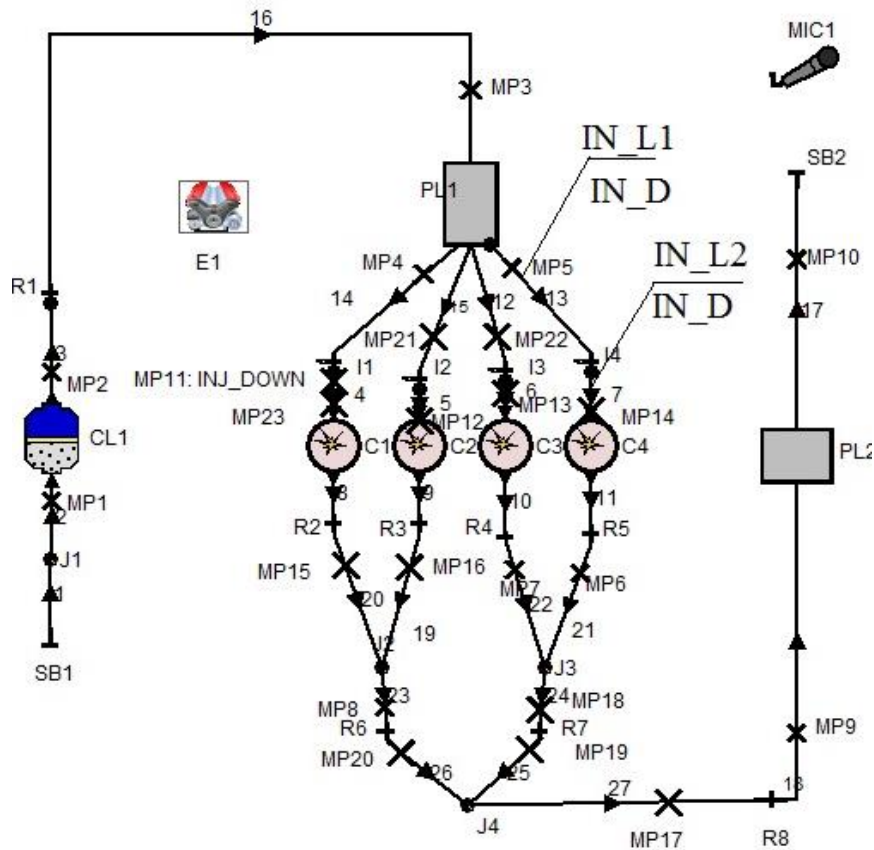

Figure 2 *1D* model of the Honda CBR 600RR (PC 37) engine.

The software also allows you to utilize a manifold model that is defined by an exact diameter for each length. The software generates its own set of elements, which may be quite accurate, slowing down the calculation. As a result, customizing your own parts will be a superior option.

The basic method used is to refine the background mesh in the region of the surfaces defined in the *STL* file, then remove cells that are external to the flow path, and finally snap the vertices of the cells to the *STL* surfaces. Control of the mesh resolution is available at various points in the meshing see figure 3.
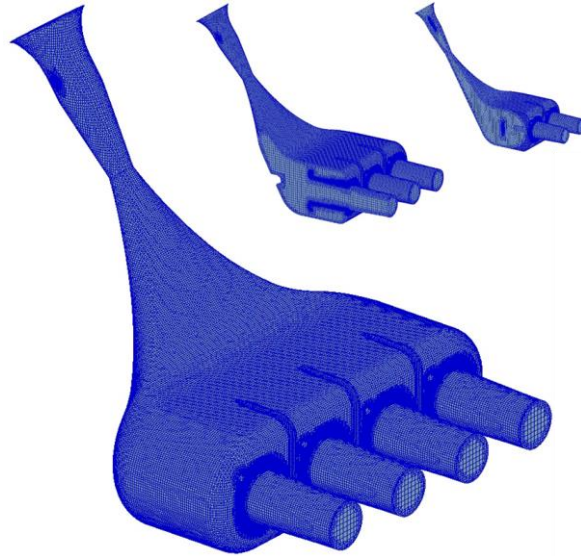
Figure 3 Intake manifold model with mesh.

From the *3D* scan of the engine, all geometric characteristics of the intake manifold and other parts of the engine were transformed into the *1D* model (such as variable diameters of the intake and exhaust pipes dependent on their length, angles in the pipe joints of the intake and exhaust manifold, materials with thermal properties , etc.).

2.2 Design of Simulations

It is necessary to perform sensitivity analysis to improve predictions based on simulation models. Table 1 a brief of input and output data were demonstrated, indicating how the system was improved.

Table 1 The data of input and output for intake system at certain operating conditions.

	Inputs					Outputs			
Simulations	Speed in rpm	Runner diameter in mm	Runner inlet length in mm	Runner outlet length in mm	Plenum vol. in liter	Power in hp	Torque in Nm	BSFC in g/kWh	SPL in dB
run 1	2000	33.5	100	100	4	11.81	42.06	396.4	90
run 2	4000	33.5	100	100	4	28	47.5	370	97
run 3	6000	33.5	100	100	4	41.81	49.63	366.6	99.8
run 4	8000	33.5	100	100	4	64.53	57.44	350.2	101.7
run 5	10000	33.5	100	100	4	86.36	61.5	350.5	103.4
run 6	2000	42	100	100	2	11.54	41.09	383.4	91
run 7	4000	42	100	100	2	28	46.5	368.2	95.8

	Inputs					Outputs			
Simulations	Speed in rpm	Runner diameter in mm	Runner inlet length in mm	Runner outlet length in mm	Plenum vol. in liter	Power in hp	Torque in Nm	BSFC in g/kWh	SPL in dB
run 8	6000	42	100	100	2	44.72	53.07	340.4	99.6
run 9	8000	42	100	100	2	58.97	52.49	356.4	101.2
run 10	10000	42	100	100	2	84.66	60.29	335.7	103
run 11	2000	32	250	100	3	11.78	41.95	397.7	91.8
run 12	4000	32	250	100	3	28	48.11	374.8	96.2
run 13	6000	32	250	100	3	47.79	56.72	365.1	100.3
run 14	8000	32	250	100	3	71.72	63.84	349.7	102.4
run 15	10000	32	250	100	3	70.58	50.26	361.4	102.2

2.3 Flow Trajectory

3D CFD analysis was performed at various stages in the design. Simulation was used to evaluate two important flow properties which is velocity and pressure. The velocity logically high in plenum zone and runner part which may lead to fluctuation in amount of air into the combustion chamber at high engine speed (figure 4, 5).
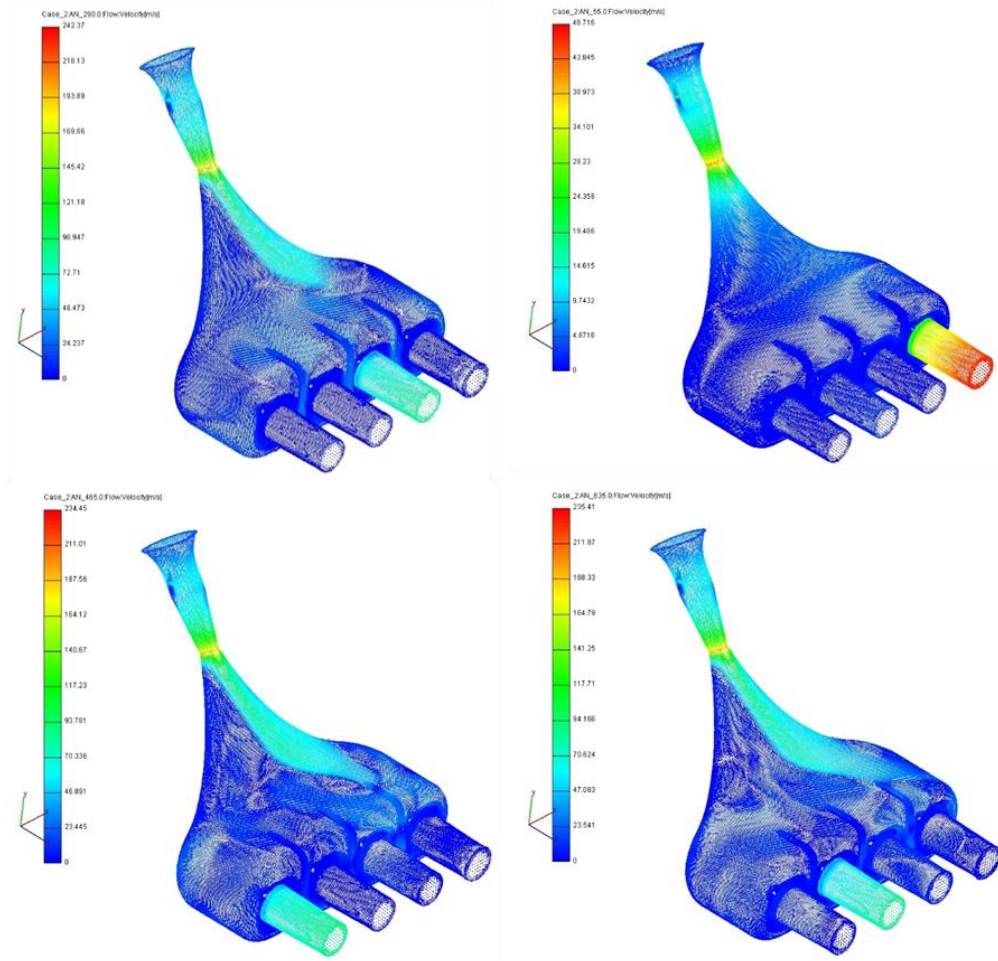

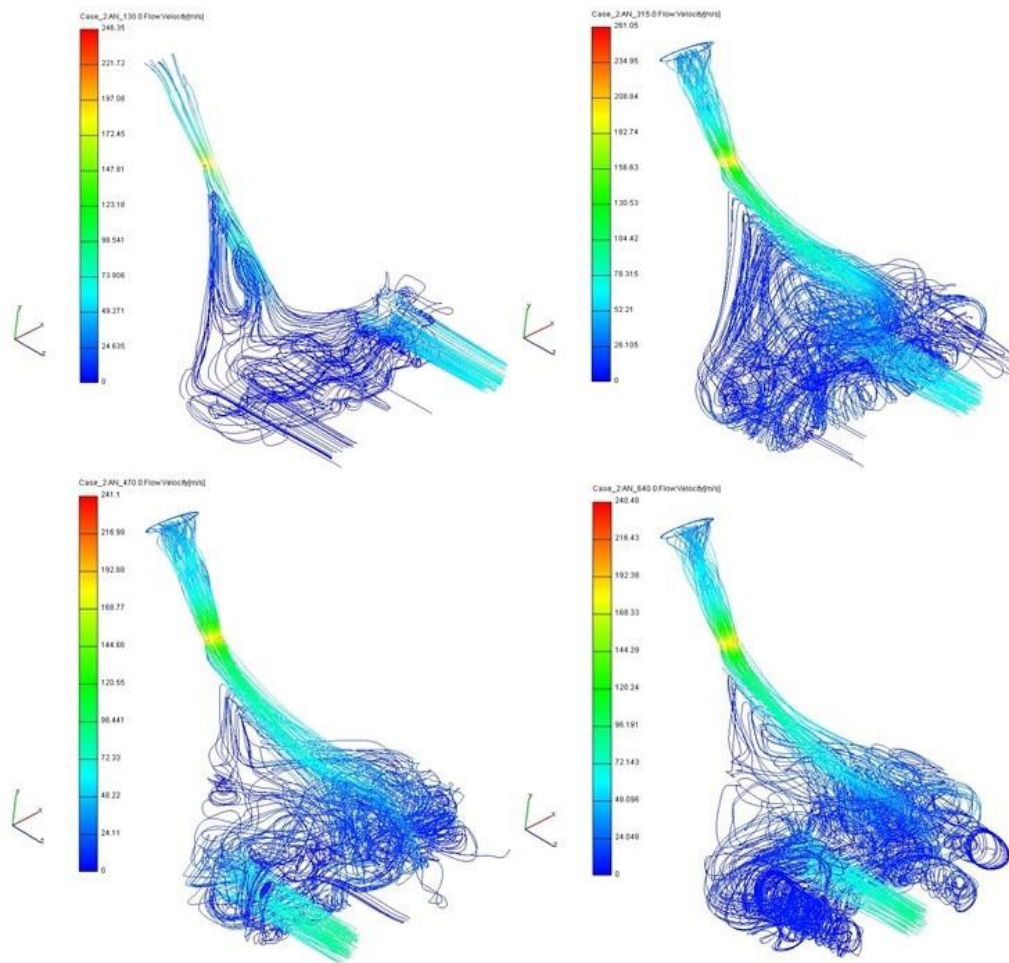Figure 4 Velocity contour *Min = 0, Max = 262.4 m/s at 8000 rpm.*

5

Figure 5 Velocity streamline *Min = 0, Max = 262.4 m/s at 8000 rpm.*

2.4 Pressure Loss

Figure 6 demonstrates the pressure and it was elevated in restriction area by *1.00036e+05 Pa at 8000 rpm*. The pressure pulsation be seen at *2000 rpm*, and have higher amplitude for *5000 rpm* than *8000 rpm*; this was mainly due to the induced frequency change of the pressure waves (reflected pressure wave) in the intake manifolds, and this is agreed with (De Risi et al. 2000) and (How Heoy Geok et al. 2009).
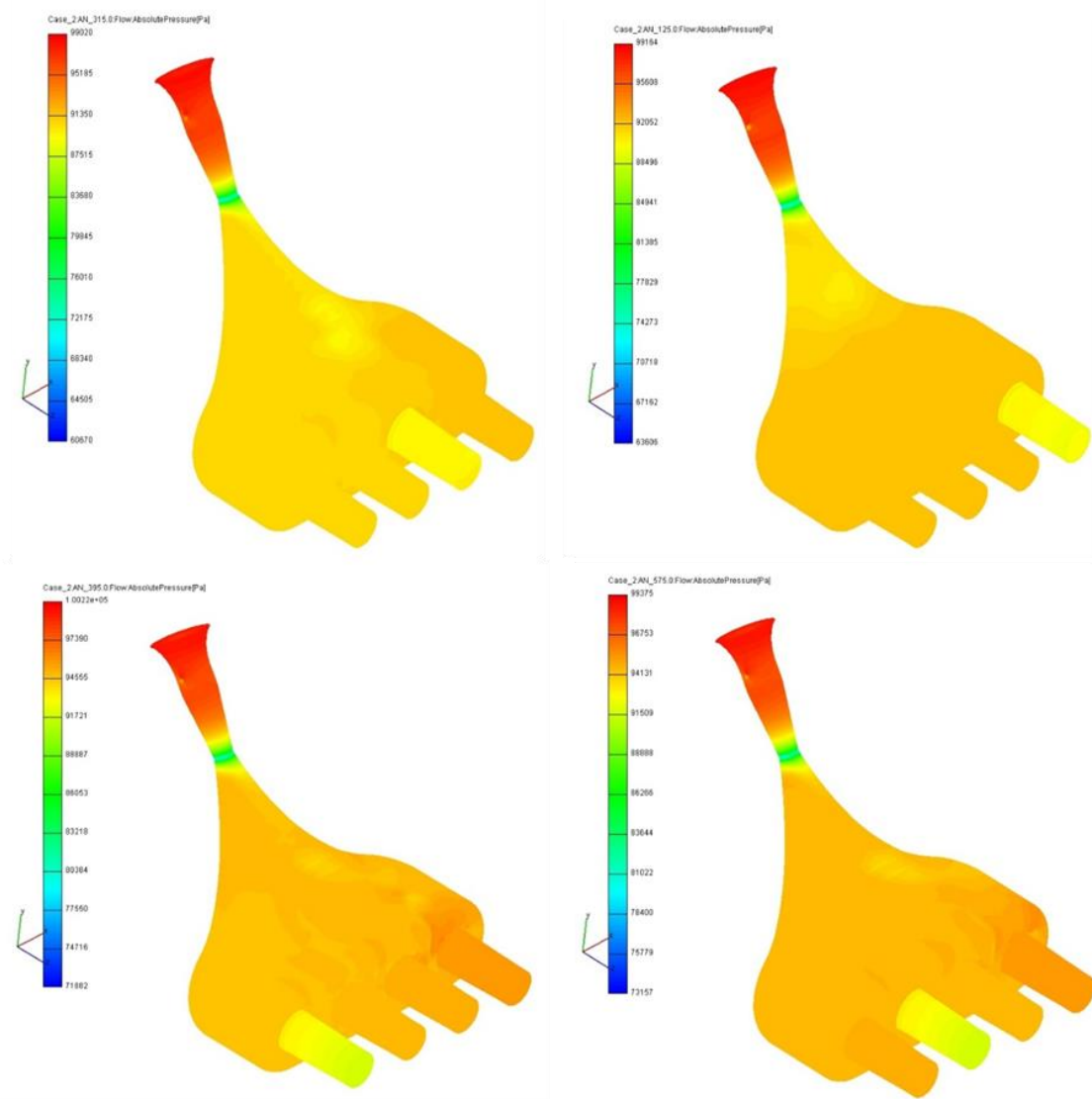
Figure 6 Pressure contour *Min = 72217, Max = 1.00036e+05 Pa at 8000 rpm.*

To be able to compare the simulation model results with the dynamometer testing results and manufacturing company data. I set every parameters of the simulation model as closest to reality as feasible.

At the purchase of the engine the salesman gave us approximate values of the torque and engine performance (engine dynos). Nevertheless, we performed the performance test at the University of Miskolc chassis dynamometer (chassis dynos). The results are shown in figure 7 along test results of two variants resulted of my research work.

The peak of power at engine speed *10500 rpm* was *78.3 hp*. This monitored the following engine calibration will be based on the data. The test shows a severe drop in power output from *6000-7500, 7500 – 10500* and *10500 - 11500 rpm* (figure 7 orange curve).
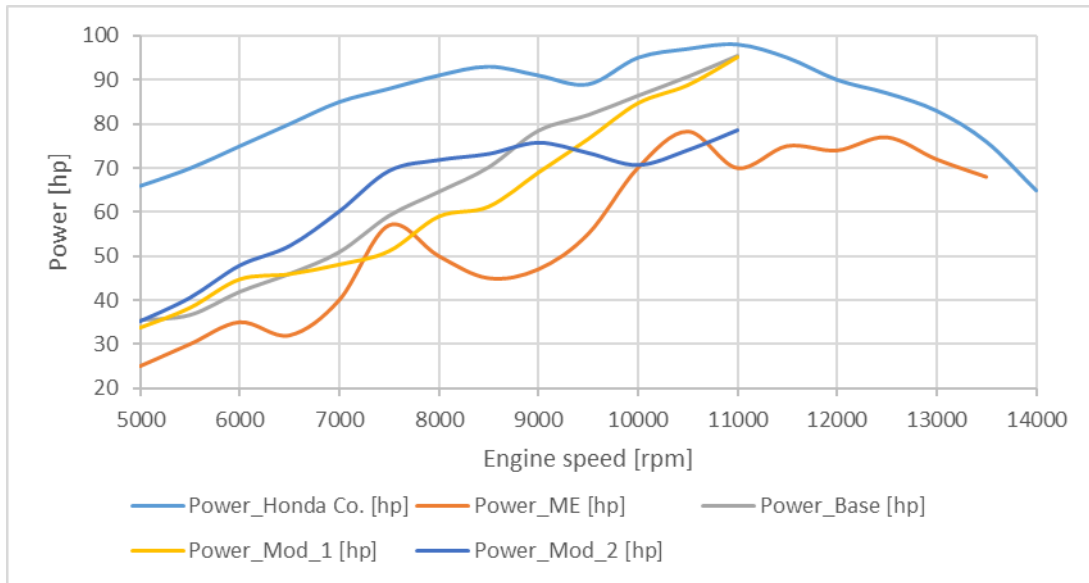
7

Figure 7 Honda CBR 600RR (PC 37) engine performance and torque recorded in manufacturing company.

The maximum torque was around *48 Nm* and *95 hp*. The results were compared with the dynamometer (Base data) and improvment suggested by simulation results (*Mod_1 and Mod_2*). There is a performance and torque characteristic of a simulation model of the Honda CBR 600RR (PC 37) engine. As its show in figure 8, the peak of torque is show up at engine speed around *11000 rpm* and its value was 48 Nm on the basis of factory data. In addition, an apparent torque loss between *12,000-14,000 rpm*. This is due to a resonance intake system that has been modified for a wider range of engine speeds.
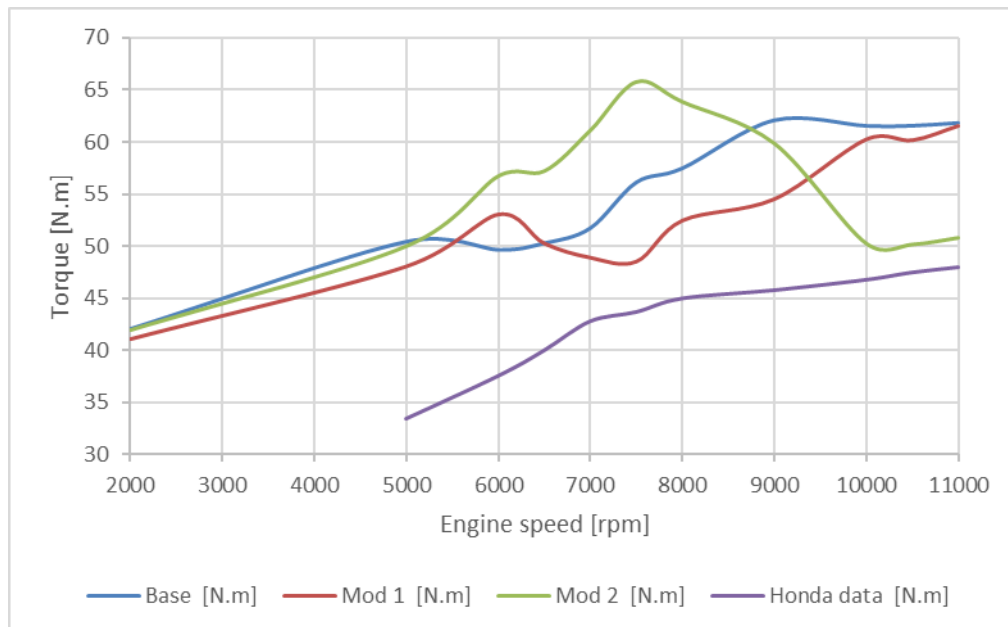

Figure 8 Honda CBR 600RR (PC 37) engine performance (Power output) recorded in University of Miskolc/Formula workshop.

3. ANALYSIS OF RACE CAR ENGINE EXHAUST SYSTEM

3.1 Structural design of formula race car exhaust system

The factory exhaust system (manifold, muffler and ducts) is made of high quality of titanium alloy, therefore the exhaust system is light-weight, and it meets all noise requirements. The term *1D* model (figure 2) implies a one-dimensional approach to the description of processes in the exhaust systems of the piston engine. The one-dimensional statement of the problem allows estimating the influence of pipelines and channels dimensions (diameters, lengths, fillet radii) on the gas flow.
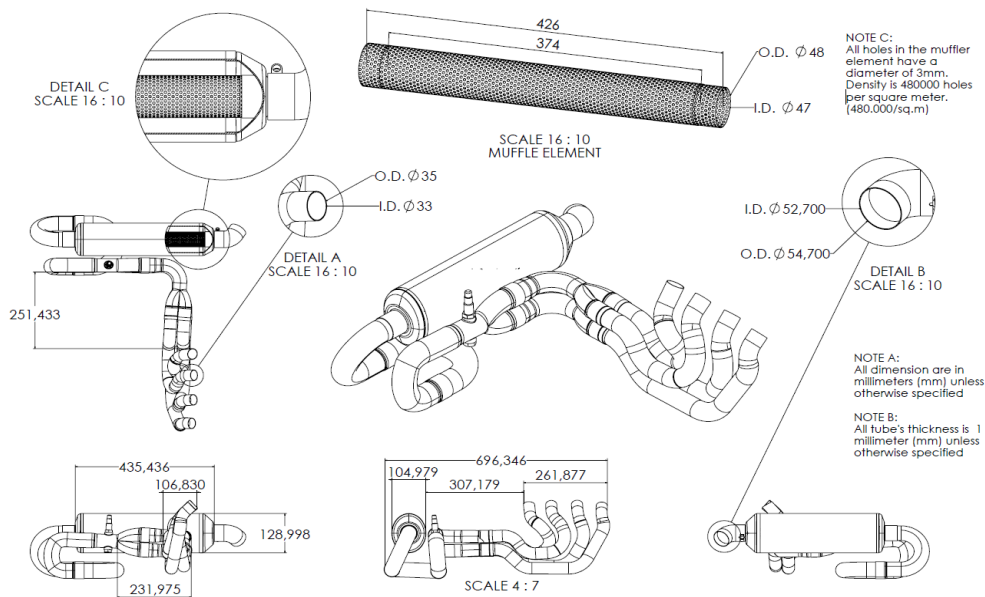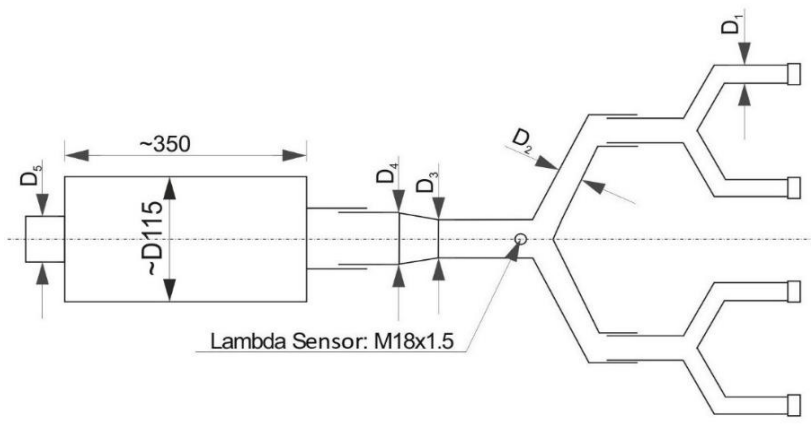

Figure 9 The porosity parameter of the perforated pipe of Honda CBR 600RR (PC 37) exhaust system.

3.2 Model description

A part of pre-processing was done using advanced design software Creo V2014, because the models are a difficult task as far as the shape is concerned and therefore, as seen in figure 9 exhaust system has to be designed in surfaces. To construct the surface model, the functions should be the multi-section surface, which draws the surface from part to part along the designed spine or guides. The dimensions were illustrated in table 2. The functions trim, revolute and extrude tools were used for the model build. The fluid volume or internal volume should be extracted due to the *CFD* simulations.

The majority of the locations in the frame consisted of sections where mating and had a small gap which means that in order to bridge that gap and make them air tight, the bridging process has to be done on each part and filled then capping the ducts. The inner volume was extracted from the solid model.

Table 2 Engine exhaust system dimensions.

Exhaust Dimensions	mm				
		1. Pipe Inside Diameter (D_1):	36	1. Pipe (D_1) Length:	420
		2. Pipe Inside Diameter (D_2):	43	2. Pipe (D_2) Length:	240
		3. Pipe Inside Diameter (D_3):	46	3. Pipe (D_3) Length:	425
		4. Pipe Inside Diameter (D_4):	48	4. Pipe (D_4) Length:	1075
		5. Pipe Inside Diameter (D_5):	52	5. Pipe (D_5) Length:	140

3.3 Exhaust manifold

Exhaust manifolds are a part of *IC* engines, they are used to collect and carry the exhaust gases away from the cylinder head and send them to the exhaust tail, with a minimum back pressure. Unstructural mesh was applied on the model as shown in figure 10 with total *2066942* of nodes and *2001883* total number of elements .
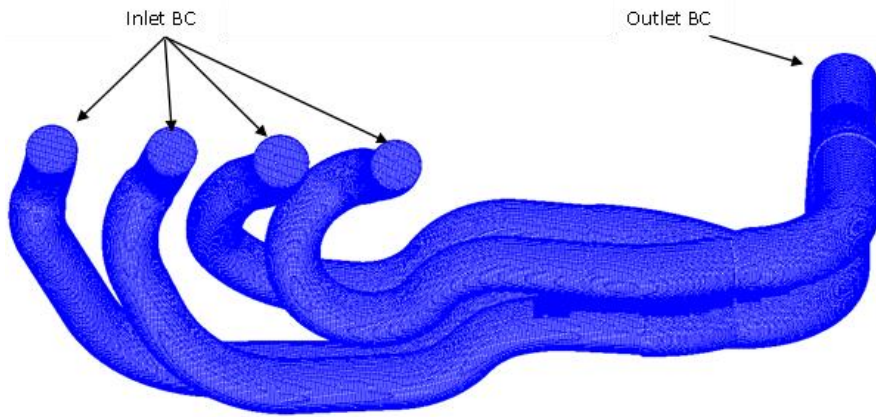

Figure 10. Control volume mesh as well as the options of the boundary conditions (*BC*).

In addition, the wall temperature of an external pipe was set $T_w = 573 \ K$, heat transfer coefficient $(h_{conv}) = 50 \ W/m^2/K$ and ambient temperature *300 K*.

10

3.4 Flow Characteristics

The flow characteristics of the exhaust manifolds of the Honda CBR 600RR (PC 37) engine were calculated using *3D* computational fluid dynamics (AVL Fire). The emitted noise has a significant impact. The pulsing flow in the duct system creates flow noise through vortex shedding and turbulence at geometrical discontinuities, which I emphasized on in this research section. Figure 11 shows an example of pressure contour at the exhaust ducts (manifold) for each stroke, maximum pessure was *1.8166e+05 at 8000 rpm.*
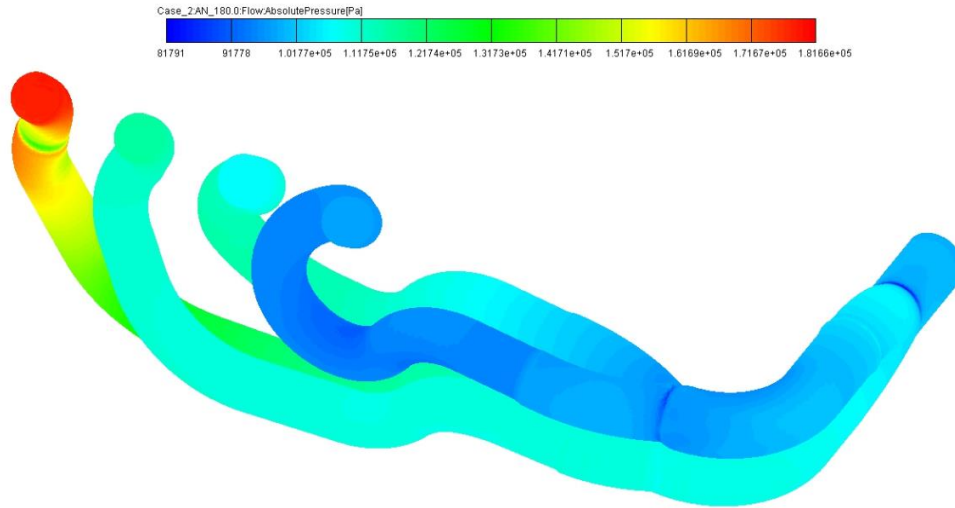

Figure 11 Exhaust manifold pressure contour at *8000 rpm.*

The dimensions and acoustic absorption qualities of the component in the exhaust line impact the propagation properties of these pulses (muffler). Noise created by high flow velocity is, in general, a disadvantage, as shown in figure 12 flow distribution may be improved with the right modification. The current findings reveal three basic distinctive factors (*E, M* and ζ) to control flow distribution and pressure drop in manifolds. However, adjustments of these parameters are not straightforward due to complexity of flow in manifolds. There is a significant difference of the friction factor and the pressure recovery factors on flow distribution. At the former half manifold, the influence of the friction factor can be neglected.
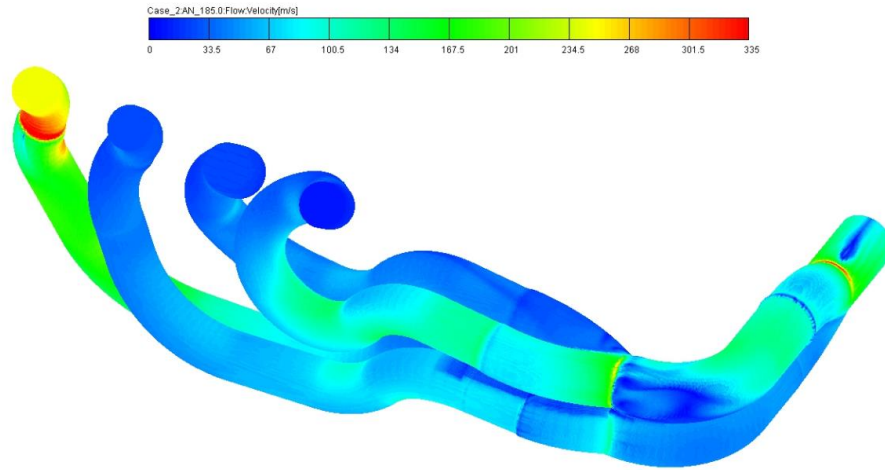
Figure 12 Exhaust manifold velocity contour at *8000 rpm.*

To generate the homogeneity structure of gas flow entering into the muffler, both bulk gas motion and turbulence characteristics of the flow are necessary. The other system variables which influence on the flow distribution are the friction slope S_f and the orifice discharge coefficient C_D. In general, the objective of uniform discharge is satisfied by ensuring that the ratio of total head variation in the manifold system to the head loss across individual outlets is kept low (figure 13). This is influenced by the ratio of manifold cross sectional area to the sum of the outlet cross-sectional areas and the spacing of the outlets. Swirl generation was identified by tracking the direction of flow vectors.
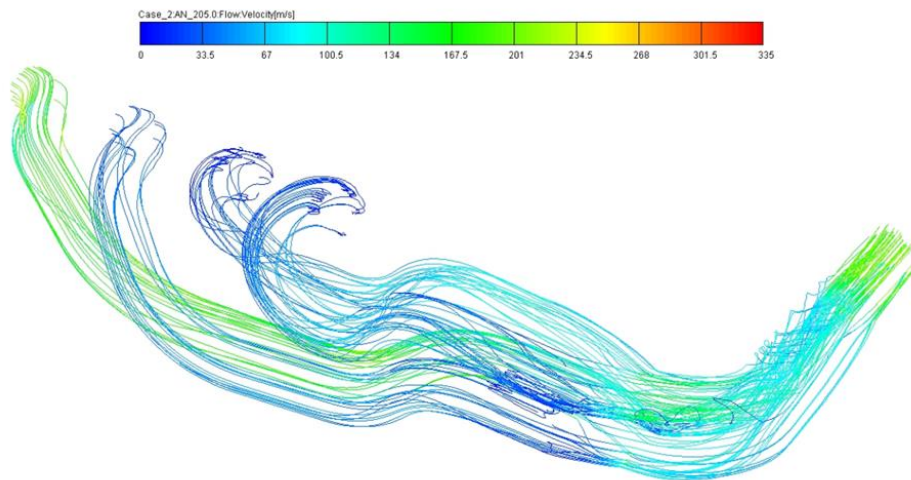
Figure 13 Exhaust manifold velocity streamline at *8000 rpm.*

3.5 Exhaust muffler

The orignal (base) muffler of Honda CBR 600RR (PC 37) is hybrid type muffler which consists of perforated pipe inside the muffler chamber (*PPiP*) and absorptive material (*AM*). When the gas flows between the chambers, through the perforated pipe, part of the acoustic energy is transformed into turbulent vortices that form at the perforations part.

The initial typical concept is quite clear to allow *3D CFD* simulation to collaborate with *1D CFD* or systems simulation (figure 14). Although the phrase zero-one-dimensional is more accurate, the term 1D approach is more commonly used, and it was used to describe the model developed in AVL Boost.
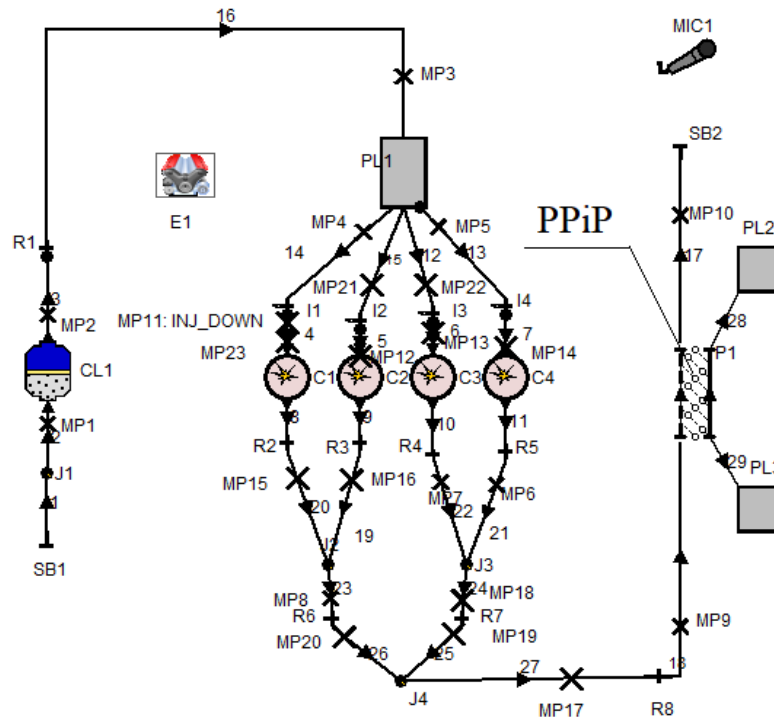

Figure 14 Scheme of Honda CBR 600RR (PC 37) engine with perforated pipe in pipe (*PPiP*) as part of muffler.

3.6 Calculation results

3.6.1 Velocity and pressure distribution in muffler

The results below adopted finite element analysis to compute the flow trajectories of the muffler. The flow rates, pressures and fluid temperatures will be communicated through the linked boundary conditions nodes throughout the solution process. The input parameters and solution status consist of *173* iterations, *201809* were fluid cells and *230933* were solid cells.

Further to this analysis, a pressure-based solver was used for visualize the flow characteristics in the muffler. The pressure field in this case is obtained through software inbuilt pressure solver, which is solving interlinked continuity and momentum equation. As show in figure 15. The maximum pressure was *102384.37 Pa* and the minimum was *100181.23 Pa* observed in the muffler without perforated tube. The non-colorful arrows represent gas flow while the colorful arrows represent reflected gas flow inside the muffler chamber. The internal pressure of the expansion chamber is relatively stable, and the distribu- tion is relatively uniform. It can be concluded that one cause of a significant elevated pressure in the

muffler part (chamber) is reflected part of gas flow at the chamber outlet. The reference values were computed from the left side (inlet).
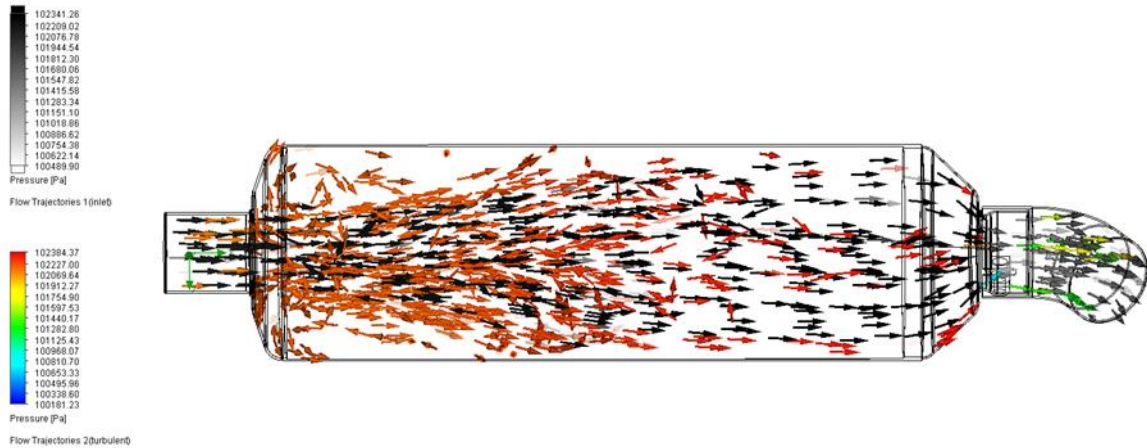

Figure 15 The volume muffler's pressure contour (flow trajectories).

Mutations in the gas flow cross-section can have a greater pressure loss. If the flow direction and the gas flow conditions change with a greater degree, it not only will generate the eddy current phenomenon, but also consume more energy. The flow velocity inside circular tube shows that there are infinite number of pulses produced. The more continuous the exhaust flow is that a fast-moving pulse creates a low-pressure area behind it. Figure 16 shows the velocity variation through different zones in geometry. It is found higher in the constrained ipipe.
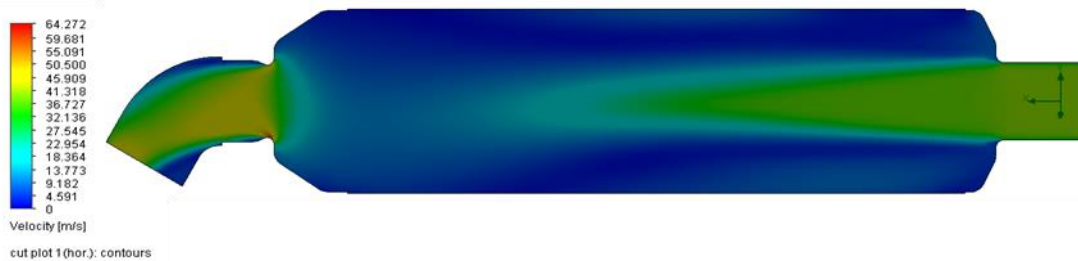
Figure 16 Velocity distribution in volume muffler.

For analyzing perforated pipe inside the muffler whose geometry is relatively complex, the computational model is split into several parts to generate mesh individually in order to decrease computational time. An element size and input information. The input parameters and solution status consist of *443* iterations, *565554* were fluid cells and *259408* were solid cells.

In the figure 17 the contour of flow field distribution of the muffler system is shown at the entrance and the exit as well. As can be seen, the largest flow velocity *(52.799 m/s)* was in the connection pipe of *PPiP* at the outlet of the muffler and the largest pressure of the body muffler (*102325.35 Pa*) was at the inlet, and minmum observed (*100778.85 Pa*) as seen in figure 17.

Figure 17 Velocity distribution in *PPiP* muffler.

As seen in figure 18 the majority of fluid in the interior of the *PPiP* muffler entered the muffler volume directly through the perforated pipe. Furthermore, 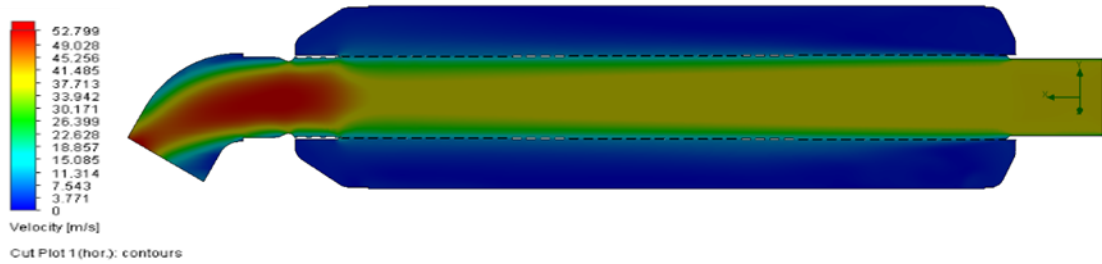the perforated tube inside the muffler featured holes with a very small diameter (*3 mm*). When fluid flowed from perforations, it was substantially reduced due to high resistance.The non-colorful arrows represent flow vector inside the perforated pipe in the muffler and the colorful arrows represent reflected flow vector or flow outside the perforated pipe.
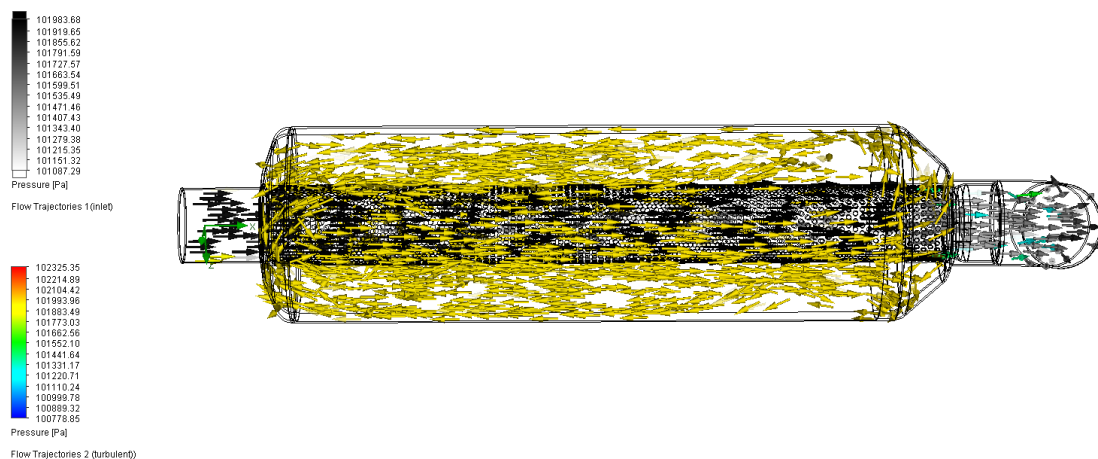
Figure 18 Pressure contour (Flow trajectories) in perforated tube and the volume part of muffler.

The pressure drop in the modeled muffler was calculated using three-dimensional calculations and the existence of an interior perforated pipe was taken into consideration. Additionally, three-dimensional models enabled the significance of Material Porosity to be clarified.

3.8 Design of Simulations

It is necessary to perform sensitivity analysis to improve predictions based on simulation models, The initial stage in the pre-processing phase is to capture a digital image of every internal component of the exhaust system before constructing a suitable mesh of these surfaces. This surface mesh is used to create the volume mesh in which the gas flows. These meshes where produced with the AVL Fire GmbH. Special attention was given to the exhaust manifold, the perforated element, and the regions where exhaust gas enters and leaves the

15

system, treated by the solver as regions of inlet and outlet. All other regions, comprising boundaries of the control volume, are defined as wall. The flow considered as turbulent within the system. Table 3 a brief of input and output data were demonstrated, indicating how the system was improved.

Table 3 The data of input and output for exhaust system at certain operating conditions.

Simulations	Inputs			Outputs			
	Speed in rpm	Pipe diameter in mm	Hole diameter in mm	Power in hp	Torque in Nm	BSFC in g/kWh	SPL in dB
run 1	2000	47	1.5	11.82	42	393	88
run 2		47	2	11.78	41.95	399	85.5
run 3		47	2.5	11.78	41.96	398	87.7
run 4		47	3.5	11.79	42	395	86
run 5		47	4	11.81	42.06	398	87.5
run 6		45	3	11.79	42	394	85.5
run 7		46	3	11.76	41.91	404	85.5
run 8		47	3	11.77	41.94	394	84
run 9		48	3	11.78	41.95	403	85
run 10		49	3	11.79	41.98	400	86
run 11		50	3	11.78	41.95	394	85

Simulations	Speed in rpm	Muffler diameter in mm	Muffler length in mm	Power in hp	Torque in Nm	BSFC in g/kWh	SPL in dB
run 12	2000	106	406	11.79	42	383	87.5
run 13		111	406	11.79	42	390	88
run 14		116	406	11.77	41.94	395	85
run 15		121	406	11.79	41.95	395	84.5
run 16		126	406	11.78	41.95	395	85
run 17		131	406	11.77	41.9	400	84.5
run 18		106	416	11.79	42	385	87.5
run 19		111	416	11.8	42	395	86
run 20		116	416	11.78	41.95	395	84.5
run 21		121	416	11.77	41.91	400	84.5
run 22		126	416	11.77	41.92	405	84.5
run 23		131	416	11.79	41.95	400	85.5

Simulations	Speed in rpm	Muffler diameter in mm	Muffler length in mm	Power in hp	Torque in Nm	BSFC in g/kWh	SPL in dB
run 24		106	426	11.79	42	395	86.5
run 25		111	426	11.78	41.95	398	86
run 26		116	426	11.77	41.94	402	85.5
run 27		121	426	11.81	42	385	87.5
run 28		126	426	11.79	42	395	86
run 29		131	426	11.79	42	395	85.5
run 30		106	436	11.78	41.95	390	85.5
run 31		111	436	11.78	41.95	395	87
run 32		116	436	11.77	41.94	402	85.5
run 33		121	436	11.79	41.95	395	86.5
run 34		126	436	11.78	41.95	395	84
run 35	2000	131	436	11.81	42	400	85.5
run 36		106	446	11.79	42	395	87
run 37		111	446	11.76	41.87	398	85.5
run 38		116	446	11.79	42	402	87
run 39		121	446	11.78	41.95	390	85
run 40		126	446	11.79	42	395	85
run 41		131	446	11.82	42.05	395	87
run 42		106	456	11.79	41.95	400	88
run 43		111	456	11.8	42	390	88
run 44		116	456	11.81	42.05	387	88
run 45		121	456	11.78	41.95	395	84.5
run 46		126	456	11.8	42	398	87
run 47		131	456	11.79	42	399	86.5

The addition of sound-absorbing material allowed for a *15-20%* reduction in *SPL* over the full engine speed range, as shown in figure 19. Meanwhile, the output flow resistance increases, lowering the engine's effective performance. Furthermore, during engine operation, the sound-absorbing material may get clogged with soot particles contained in the exhaust gases, resulting in an increase in resistance at the outlet and a worsening of the engine's operating conditions.

In the engine cylinders, the combustion process was modeled. It is also feasible to represent the production of soot in the applicable model, although for *SI* engines with external mixing, soot emissions may be ignored. Afterburning processes are not replicated in the exhaust system, and the temperature of exhaust gases changes due to heat exchange with the environment. A primary muffler also had a lower mass while maintaining adequate the lowest *SPL* at the output end, which was a multi-objective optimization challenge. The commercial software was used for all optimization stages.
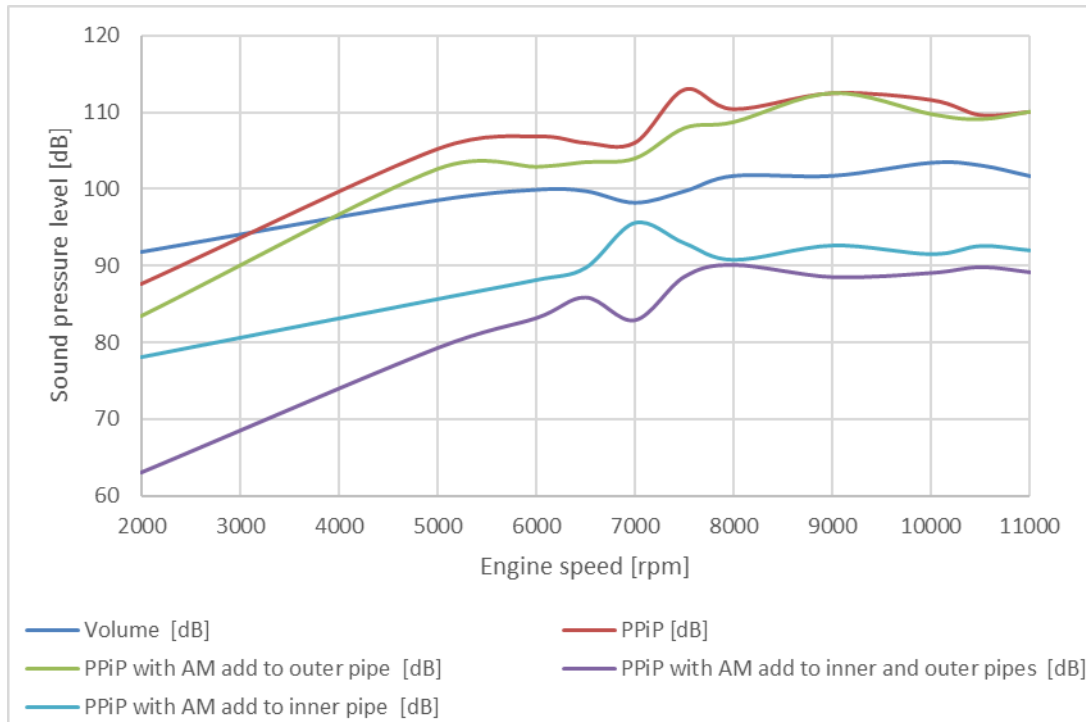
Figure 19 *FS* engine sound pressure level with different types of muffler materials; (*AM*) refer to absorbing material.

The parameters of *AM*: *porosity = 0.9* and *flow resistivity = 10000 N·s/m⁴*. The material porosity represents the fraction of air space within the material (*0 to 1*). This will be a function of the packing density of the material. For example, a Material Porosity of *0.9* defines that *10%* of the volume is filled with material and *90%* is space for the gases.

A rigorous two-load approach is adopted to analyze the acoustic performance of a cylindrical muffler whose walls are treated with a locally reacting absorbent liner. The expansion chamber is separated from the central airway which contain a uniform main gas flow by a perforated cylindrical tube. The effect of the perforated center tube is modelled as a partially transmitting surface characterized by the boundary conditions.
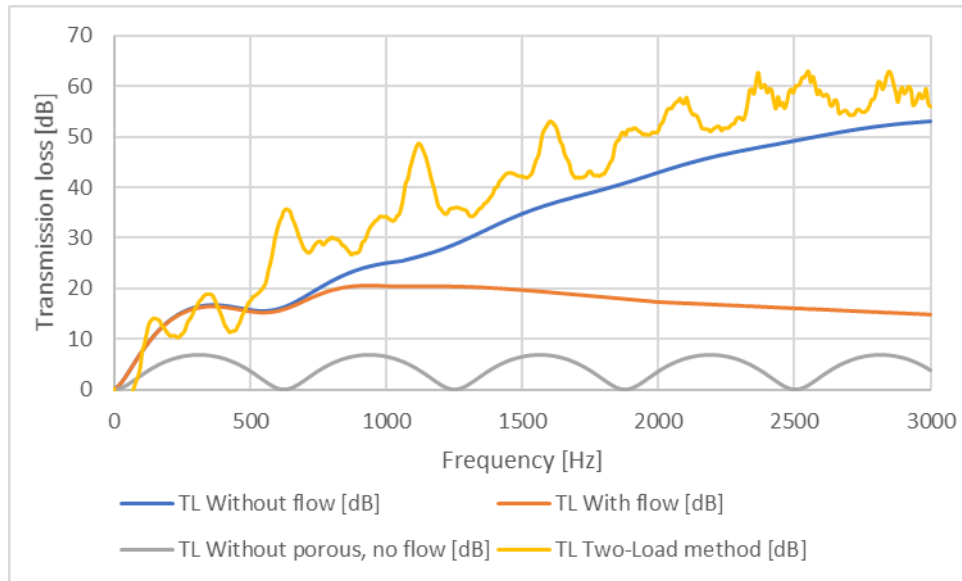
Figure 20 Comparison of Transmission loss calculated for several cases.

Figure 20 presents a comparison of experimental and numerical techniques by concentrating on the transmission loss result of the muffler over frequency. Hybrid mufflers are usually effective in both the low and high frequency ranges. The exhaust flow field was addressed differently using analytical methods, the results include 4 cases:

- Case-1: Indicates the *TL* calculated by the analytical approach, based on *1D* wave model without flow.
- Case-2: Indicates the *TL* calculated by the analytical approach, *1D* wave model with flow.
- Case-3: Indicates the *TL* calculated by the analytical approach, *1D* wave model of the muffler volume (without *PPiP*).
- Case-4: Presents the *TL* graph measured by two-load method and performed without the flow.

In experimental result the frequency ranges from *400-700 Hz*, the maximum attenuation was *35 dB* for perforations part (PPiP), as well as for the frequency range *2400-2600 Hz* has reached a maximum *TL* of *61 dB*. In fact. However, *TL* for the basic (current) hole diameter of the FS muffler at high porosity appears to diminish, which is agree with (Lee and Selamet, 2006). The diffrence in geometry between the two, but the geometry without perforated tube of normal mode goesifar beyond indicating that this does not improve the transmission loss feature.

Finally, it is to be mentioned that the proposed method (the result related to the case *1* and case *2*) are not applicable for porous materials with low flow resistivity and/or small thickness (*d*). The acoustic resistance depends on the flow through the perforate holes.   On the other hand, perforates can deteriorate the engine performance, if badly designed, by increasing the flow back pressure.

3 NEW SCIENTIFIC RESULTS – THESES

T1. As a result of my investigations, I proposed and utilized a complex simulation technique which connects the advantages both of the *1D* acoustic simulation and *3D CFD* simulation. Based on the combined calculation process I was able to handle the acoustic performance of the intake and exhaust system components of a race car engine and the procedure can be repeated for any other flow related problem.

T2. An extensive sensitivity analysis based on the proposed technique from *T1* was performed in order to obtain the best muffler geometry for the best acoustic performance. I proved that for the analysed geometry parameters of the muffler with the used parameter ranges of *Lm* (length of pipe), *Dm_out* (muffler outer diameter) *Dm_in* (perforated pipe diameter), *D_hole* (perforation hole diameter) an optimum solution related to the best acoustic performance (orifice noise) can be selected precisely for the *FS* car.

T3. As result of my investigations, I showed that the proposed combined simulation method is able to optimize engine parameters (such as brake specific fuel consumption, engine power and torque) through muffler geometry modification, despite the main focus is on the orifice noise reduction.

T4. I proved through my investigations that by using the Johnson–Champoux–Allard (*JCA*) model in case of absorptive material in the muffler, the simulation with the given parameters delivers sufficient results for the transmission loss of a muffler compared to the test rig measurement. With the proposed simulation method incl. *JCA*, I proved that the transmission loss over the frequency of a muffler can be predicted in a good confidence range.

4   LIST OF PUBLICATIONS RELATED TO THE TOPIC OF THE RESEARCH FIELD

IN ENGLISH

(1)   Mohamad, B., Szepesi, G., & Bolló, B. (2017). *Combustion Optimization in Spark Ignition Engines*. Multi-Science - XXXI. microCAD Scientific Conference. University of Miskolc-Hungary. DOI:10.26649/musci.2017.065.

(2)   Mohamad, B., Szepesi, G., & Bolló, B. (2017). *Review Article: Modelling and Analysis of a Gasoline Engine Exhaust Gas Systems.* International Scientific Conference on Advances in Mechanical Engineering. University of Debrecen-Hungary.

(3)   Mohamad, B., Szepesi, G., & Bolló, B. (2018). *Review Article: Effect of Ethanol-Gasoline Fuel Blends on the Exhaust Emissions and Characteristics of SI Engines.* Lecture Notes in Mechanical Engineering. 29-41. https://doi.org/10.1007/978-3-319-75677-6_3

(4)   Mohamad, B., & Amroune, S. (2019). *The analysis and effects of flow acoustic in a commercial automotive exhaust system.* Advances and Trends in Engineering Sciences and Technologies III: Proceedings of the 3rd International Conference on Engineering Sciences and Technologies (ESaT 2018), September 12-14, 2018, High Tatras Mountains, Tatranské Matliare, Slovak Republic. pp. 197-202.

(5)   Mohamad, B., Karoly, J., & Kermani, M. (2019). *Exhaust System Muffler Volume Optimization of Light Commercial passenger Car Using Transfer Matrix Method.* International Journal of Engineering and Management Sciences. 4, (1). Pp. 132-139. DOI: 10.21791/IJEMS.2019.1.16.

(6)   Mohamad, B., Karoly, J., Zelentsov, A. (2019). *Investigation and optimization of the acoustic performance of formula student race car intake system using coupled modelling techniques,* Design of Machines and Structures, 9, (1), pp.13-23. DOI: 10.32972.dms.2019.002.

(7)   Mohamad, B., (2019). *A review of flow acoustic effects on a commercial automotive exhaust system.* Mobility &Vehicle Mechanics Mobility &Vehicle Mechanics, 45, (2), pp 1-14. DOI:10.24874/mvm.2019.45.02.01.

(8)   Mohamad, B., (2019). *A review of flow acoustic effects on a commercial automotive exhaust system-methods and materials.* Journal of Mechanical and Energy Engineering, 3, (2), pp. 149-156, DOI:10.30464/jmee.2019.3.2.149.

(9)   Mohamad, B. (2019). *Design and Optimization of Vehicle Muffler Using The Ffowcs Williams and Hawkings Model*. Machine Design Journal, 11, (3), pp. 101-106. DOI: 10.24867/MD.11.2019.3.101-106.

(10) Mohamad, B., Zelentsov, A. (2019). *1D and 3D Modeling of Modern Automotive Exhaust Manifold.* Journal of the Serbian Society for Computational Mechanics, 13, (1), pp.80-91. DOI: 10.24874/jsscm.2019.13.01.05.

(11)   Mohamad, B., Karoly, J., & Zelentsov, A. (2020). *CFD Modelling of Formula Student Car Intake System.* Facta Universitatis, Series: Mechanical Engineering, 18, (1), pp. 153-163. https://doi.org/10.22190/FUME190509032M.

(12)   Mohamad, B., Ali, M.Q., Neamah, H.A., Zelentsov, A., Amroune, S. (2020). *Fluid dynamic and acoustic optimization methodology of a formula-student race car engine exhaust system using multilevel numerical CFD models.* Diagnostyka, 21, (3), pp. 103-113. DOI:10.29354/diag/126562.

(13)   Mohamad, B., Karoly, J., Zelentsov, A., & Amroune, S. (2020). *A hybrid method technique for design and optimization of Formula race car exhaust muffler.* International Review of Applied Sciences and Engineering, 11, (2), pp. 174–180. https://doi.org/10.1556/1848.2020.20048.

(14)   Mohamad, B., Karoly, J., Zelentsov, A., & Amroune, S. (2021). *A Comparison Between Hybrid Method Technique and Transfer Matrix Method for Design Optimization of Vehicle Muffler.* FME Transactions. 49, (2), pp. 494-500. DOI: 10.5937/fme2102494M.

IN HUNGARIAN

(1)   Mohamad, B., Karoly, J., Zelentsov, A. (2019). *Hangtompító akusztikai tervezése hibrid módszerrel.* Multidiszciplináris Tudományok, 9, (4), pp. 548-555. DOI: https://doi.org/10.35925/j.multi.2019.4.58.

IN RUSSIAN

(1)   Мохамед, Б., Кароли, Я., & Зеленцо, А. (2020). *Трехмерное моделирование течения газа во впускной системе автомобиля «Формулы Студент»* Журн. Сиб. федер. ун-та. Техника и технологии, 13, (5), pp. 597-610. DOI: 10.17516/1999-494X- 0249.

5 LITERATURE CITED IN THE THESES BOOKLET

[1] Krebber, W., Genuit, K., & Sottek, R. (2002). *Sound quality of vehicle exterior noise*. In Proceeding of Forum Acusticum.

[2] García, A., & Faus, L. (1991). *Statistical analysis of noise levels in urban areas*. Applied Acoustics, v. 34, n. 4, 227 – 247.

[3] Juraga, I., Paviotti, M., & Berger, B. (2015). *The environmental noise directive at a turning point*. In Proceedings of EuroNoise Conference (2015, Maastricht, The Netherlands), pp. 1041–44.

[4] De Risi, A., Zecca, R., & Laforgia, D. (2000). *Optimization of a Four Stroke Engine by Means of Experimental and 1-D Numerical Analysis*. SAE Technical Paper. 2000-01-0566. https://doi.org/10.4271/2000-01-0566.

[5] How Heoy Geok, Taib Iskandar Mohamad, Shahrir Abdullah, Yusoff Ali, & Azhari Shamsudeen. (2009). *Experimental Investigation of Performance and Emissions of a Sequential Port Injection Compressed Natural Gas Converted Engine*. SAE Technical Papers. 2009-32-0026

[6] Lee I., & Selamet A. (2006). *Impact of perforation impedance on the transmission loss of reactive and dissipative silencers*. The Journal of the Acoustical Society of America. 120, 3706. https://doi.org/10.1121/1.2359703.